Experimental Study on Curing of Ultrafine Tailings Sand Based on an Orthogonal Test

Yueqi Shi[1,2,*], Changhong Li[1,2], Zhiwen Song[1,2] and Peng Liu[1,2]

[1]School of Civil and Resource Engineering, University of Science and Technology Beijing(USTB), Beijing 100083, China
[2]Beijing Key Laboratory Of Urban Underground Space Engineering USTB, Beijing 100083 China
a. syq_shi@126.com
**Yueqi Shi*

Keywords: Ultrafine tailings, solidification, orthogonal test, strength characteristics.

Abstract: Due to the continuous improvement of the beneficiation process, the grain size of the tailings sand is decreasing day by day. The proportion of the total tailings of many mines below the 74um particle size exceeds 50%, These pose new challenges to the stability of the tailings sand during the storage process.. This paper takes the tailings sand of Chenkeng tailings reservoir area under the pit of Mukeng Mining Company as the research object, and selects the different ratios of cement cement, fly ash, blast furnace slag and desulfurization gypsum as test variables. For the experimental variables, the curing orthogonal test was carried out to comprehensively analyze the effects of various levels on the solidification effect of tailings sand. The results show that: (1) the cohesion and internal friction angle of the sample after 7 days of curing In terms of comprehensive consideration of the main influencing factors of the two, the best curing agent ratio is 3% of cement clinker, 1.5% of fly ash, 2% of blast furnace slag, and 1% of desulfurized gypsum. After the agent, the cohesive force of the ultrafine tailings sand is raised from the original 27.00 kPa to 50.53~161.94 kPa, and the internal friction angle is raised from the original 25.53° to 29.41~35.58°. The solidified tailings sand sample Cohesion and its uniaxial compressive strength There is a certain positive correlation between degrees. (2) When the content of curing agent is between 4.5 and 7%, the permeability coefficient of the cured sample will continue to decrease, but the decreasing trend will gradually slow down. The permeability coefficient of the sample after curing was measured to be between 5.00×10-6~1.61×10-5 cm/s.

1. Introduction

At present, in the concentrating plants that have been put into production or under construction at home and abroad, the final product particle size of 53μm or less has become more common, and the final product size of some selected plants has even reached 30μm [1]. The ultrafine particle size tailings are in the process of discharge and storage. A series of technical problems and environmental problems have arisen. Due to the large amount of emissions and low utilization rate of tailings, a large number of tailings can only be accumulated in the tailings pond. The tailings pond refers to the dam blocking the valley mouth or The site consisting of the surrounding area for

stockpiling mines to remove tailings after ore sorting is a source area with high potential energy and is a major source of danger. Once the tailings dam breaks, the water body and near saturation in the reservoir area The tailings will overflow and make the life and property of the downstream people safe and the ecological environment around the reservoir area threatened [2, 3, 4, 5, 6, 7, 8].

In this paper, four kinds of cementitious materials such as cement clinker, fly ash, blast furnace slag and desulfurization gypsum are used to develop a new type of curing agent. The four components are used as experimental factors to carry out the orthogonal test of tailings sand solidification, combined with the soil mechanical parameters. Determine and verify the solidification effect of tailings sand to reach the purpose of controlling the hidden danger of tailings dam. Cement clinker, blast furnace slag and fly ash are common cementing materials, when added in the reaction system containing these three In the case of gypsum, it will form hydrated calcium sulphoaluminate with the hydration product. These products can coagulate and harden in the air and continue to harden in water, with a relatively high strength. The presence of calcium hydroxide and gypsum makes the active mixed material The potential activity is exerted, that is, calcium hydroxide and gypsum act to stimulate hydration and promote coagulation hardening, so it is called an activator [9, 10, 11, 12].

2. Basic Properties of Ultrafine Tailings Sand

2.1.Phase Composition of Ultrafine Tailings Sand

According to the XRD test, the phase composition of the ultrafine tailings sand is: calcite (chemical formula $CaCO_3$), calcium garnet (Andradite, chemical formula Ca_3Fe_2 (SiO_4) $_3$), quartz (Quartz, chemical formula SiO_2), fluorite (Fluorite, chemical formula CaF_2) and vermicite (Titanite, chemical formula $CaTiOSiO_4$), as shown in Figure 1.

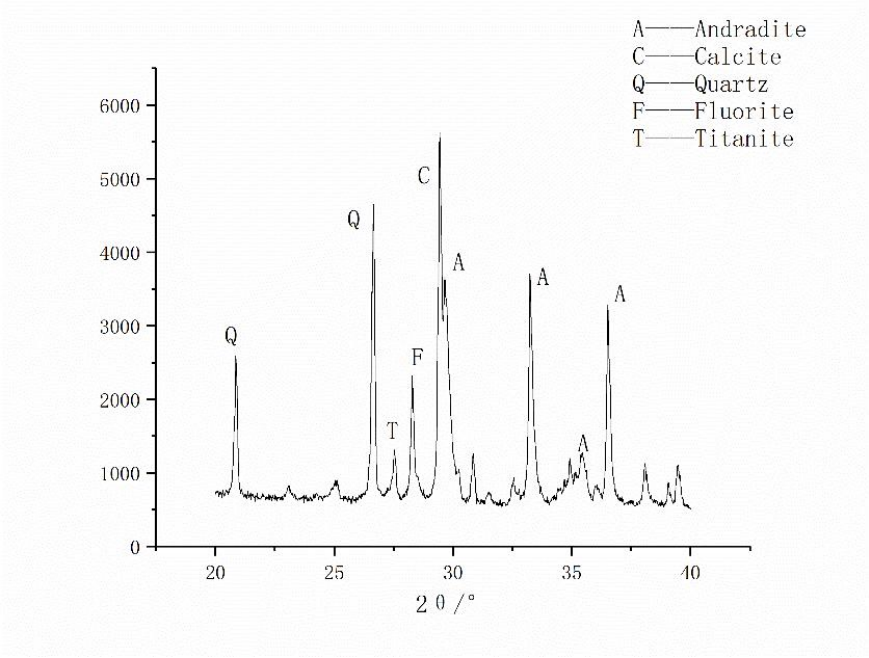

Figure 1: XRD pattern of ultrafine tailings.

The contents of each substance are shown in Table 1.

Table 1: Mineral composition and content of ultrafine tailings.

Mineral composition	Calcite	Andradite	Quartz	Fluorite	Titanite
Content/%	25.6	43.3	16.4	7.3	7.4

2.2.Soil Mechanics Parameters of Ultrafine Tailings

The original ultrafine tailings were tested for saturated water content, saturation density, dry density, permeability coefficient test and direct shear. The results are shown in Table 2.

Table 2: Soil mechanical parameters of ultrafine tailings sand.

Parameter Name	Value
Saturated water content	15.15%
Saturated density	2.61 g/cm^3
Dry density	2.27 g/cm^3
Coefficient of permeability	4.03×10^{-05} cm/s
Cohesion	27.0kPa
Internal friction angle	25.53°

3. Analysis of Curing Test of Ultrafine Tailings

3.1.Unconfined Compressive Strength Test

The orthogonal test of the curing test with a curing age of 7 days is shown in Table 3.

Table 3: Orthogonal table of curing test with curing age of 7 days.

Test number	A Clinker (%)	B Fly ash (%)	C Blast furnace slag (%)	D Desulphuri-zation gypsum (%)	Compressive strength (MPa)
1	(1)2.00	(1)1.00	(1)1.00	(1)0.50	0.19
2	(1)2.00	(2)1.50	(2)1.50	(2)0.75	0.24
3	(1)2.00	(3)2.00	(3)2.00	(3)1.00	0.33
4	(2)2.50	(1)1.00	(2)1.50	(3)1.00	0.25
5	(2)2.50	(2)1.50	(3)2.00	(1)0.50	0.34
6	(2)2.50	(3)2.00	(1)1.00	(2)0.75	0.23
7	(3)3.00	(1)1.00	(3)2.00	(2)0.75	0.30
8	(3)3.00	(2)1.50	(1)1.00	(3)1.00	0.23
9	(3)3.00	(3)2.00	(2)1.50	(1)0.50	0.29
K1	0.76	0.74	0.64	0.82	.
K2	0.82	0.81	0.78	0.76	
K3	0.82	0.85	0.96	0.81	
k1	0.25	0.25	0.21	0.27	
k2	0.27	0.27	0.26	0.25	
k3	0.27	0.28	0.32	0.27	
R	0.02	0.04	0.11	0.02	

Use the K1 value in the first column to indicate the sum of the test indicators under the A1 condition, which is the sum of the compressive strengths at level 1 in the first column.

K1 (column 1)=0.19+0.24+0.33=0.76(Mpa)

For the same reason, K2 and K3 in the first column can be used to represent the sum of the test indicators under the conditions of A2 and A3.

K2 (column 1) = 0.25 + 0.34 + 0.23 = 0.82 (Mpa)

K3 (column 1) = 0.30 + 0.23 + 0.29 = 0.82 (Mpa)

At this time, k1, k2, and k3 can be used to represent the average values of K1, K2, and K3, respectively.

Similarly, the calculation results of the K value and the k value in the second column, the third column, and the fourth column can be counted in Table 3, respectively.

In order to more intuitively determine the influence of the horizontal change of each factor on the compressive strength value, the factor level is taken as the abscissa, the compressive strength is the ordinate, and the relationship between the factor level and the compressive strength value is plotted.

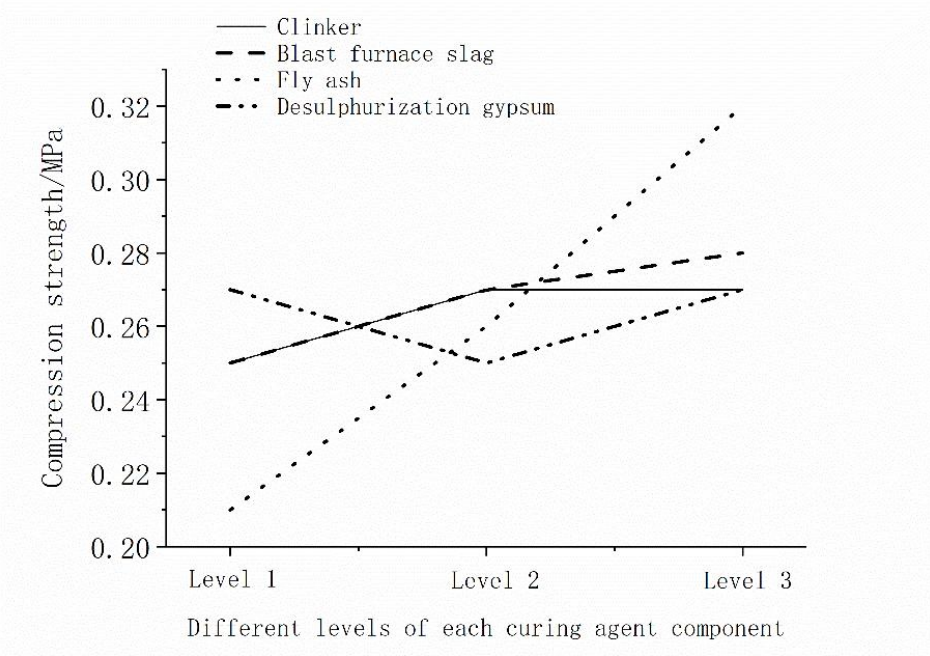

Figure 2: Relationship between different levels of curing agent

content and compressive strength values (7 days).

From Table 3 or from Figure 2, it can be seen that the average compressive strength value is maximized, and the factors selected by each factor are: cement clinker content of 3% (A3), and fly ash content of 2 % (B3), the content of blast furnace slag is 2% (C3), and the content of desulfurization gypsum is 1% (D1). The ideal condition is: A3B3C3D1.

At the same time, in order to determine the main influencing factors affecting the compressive strength value, it is necessary to compare the extreme value of the compressive strength value caused by the change of the level of each factor, which is represented by the letter R. The calculation process is as follows:

R (column 1) = 0.27-0.25 = 0.02 (MPa)

R (column 2) = 0.28-0.25 = 0.03 (MPa)

R (column 3) = 0.32 - 0.21 = 0.11 (MPa)

R (column 4) = 0.27-0.25 = 0.02 (MPa)

The magnitude of the range reflects the degree of influence of the change of the factor on the value of the compressive strength. The greater the difference, the greater the degree of influence. Therefore, the above-mentioned range reflects the degree of influence in this test:

C→B→A→D

On the whole, the 7 days test block has a tendency to increase the compressive strength value with the increase of cement clinker, fly ash and blast furnace slag content. For desulfurization gypsum, the content change is for compressive pressure. The effect of the intensity value is not obvious. The optimal level combination of each factor is: A3B3C3D1.

Further analysis, it can be found that for cement and fly ash, the influence of the increase of the content on the compressive strength value of the test piece is gradually reduced. For the blast furnace slag, the compressive strength value has obvious as the content increases. Improved, and basically linear relationship.

3.2.Direct Shear Test

The cohesion and internal friction angles were obtained by direct shear test on the cured ultrafine tailings, as shown in Table 4.

Table 4: Direct shear test record table for cured samples.

Test number	A Clinker (%)	B Fly ash (%)	C Blast furnace slag (%)	D Desulphuri-zation gypsum (%)	Cohesion (kPa)	Internal friction angle (°)
1	(1)2.00	(1)1.00	(1)1.00	(1)0.50	50.53	29.41
2	(1)2.00	(2)1.50	(2)1.50	(2)0.75	74.81	35.58
3	(1)2.00	(3)2.00	(3)2.00	(3)1.00	117.16	32.33
4	(2)2.50	(1)1.00	(2)1.50	(3)1.00	101.33	35.17
5	(2)2.50	(2)1.50	(3)2.00	(1)0.50	140.70	33.63
6	(2)2.50	(3)2.00	(1)1.00	(2)0.75	82.71	30.78
7	(3)3.00	(1)1.00	(3)2.00	(2)0.75	129.74	31.95
8	(3)3.00	(2)1.50	(1)1.00	(3)1.00	81.42	33.45
9	(3)3.00	(3)2.00	(2)1.50	(1)0.50	161.94	30.00

At this time, since there are two judgment indicators, the “integrated balance method” can be used in the analysis. The comprehensive balance method analyzes each indicator according to a single indicator, and then comprehensively balances the calculation and analysis results of each indicator. Conclusions In this group of experiments, the indicator test analysis table can be obtained from Table 4, as shown in Table 5.

Table 5: Indexes analysis table of direct shear test.

Index	Cohesion (kPa)				Internal friction angle (°)			
Factor	A	B	C	D	A	B	C	D
K1	242.50	281.60	214.65	353.17	97.32	96.53	93.64	93.04
K2	324.74	296.94	338.08	287.26	99.58	102.66	100.75	98.31
K3	373.10	361.81	387.60	299.91	95.40	93.11	97.91	100.95
k1	80.83	93.87	71.55	117.72	32.44	32.18	31.21	31.01
k2	108.25	98.98	112.69	95.75	33.19	34.22	33.58	32.77
k3	124.37	120.60	129.20	99.97	31.80	31.04	32.64	33.65
R	43.53	26.74	57.65	21.97	1.39	3.18	2.37	2.64

From Table 5, the relationship between the cohesive force and the internal friction angle with respect to different levels of each factor can be plotted, as shown in Figs.

The primary and secondary relationships of these four factors for the two indicators are as follows:

Cohesion: C→A→B→D

Internal friction angle: B→D→C→A

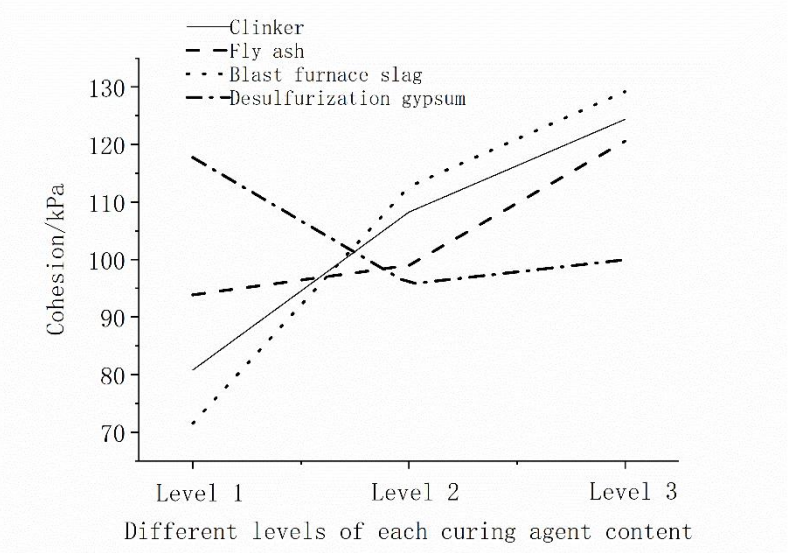

Figure 3: Relationship between different levels of curing agent content and cohesion (7 days).

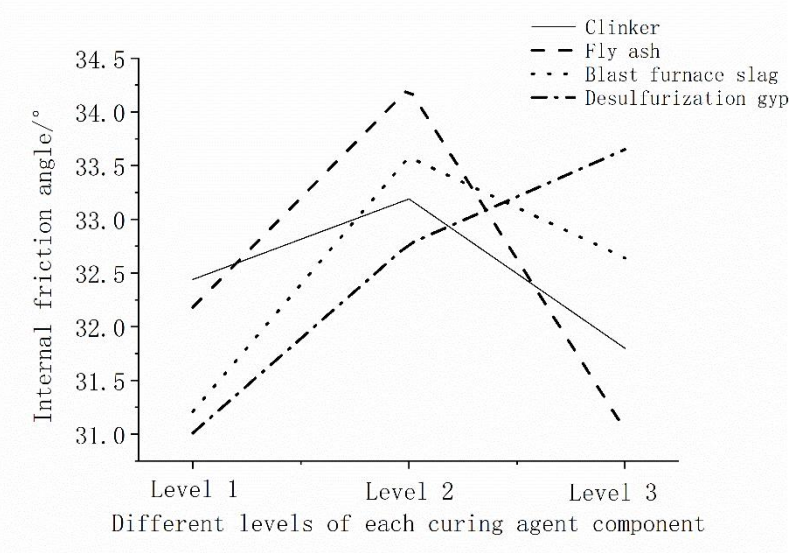

Figure 4: Relationship between different levels of curing agent

content and cohesion internal friction angle (7 days).

From the calculation and analysis of various indicators, the best condition of the index of cohesion in this group of tests is A3B3C3D1; the best condition of internal friction angle in this group of tests is A2B2C2D3. The optimal conditions are inconsistent, so it is necessary to determine the appropriate conditions by analyzing the influence of each factor on the two indicators. From Table 5, it can be calculated that for the cohesion force, the column R and all the samples are The ratio α of the cohesion mean value is shown in Table 6(a). It can also be calculated that the ratio of the range R of the internal friction angle to the mean value of the internal friction angle of all the samples is shown in Table 6(b).

Table 6(a): Ratio table of range and mean value (cohesion).

Mean value of cohesion /kPa	104.48			
R/kPa	43.53	26.74	57.65	21.97
α	0.42	0.26	0.55	0.21

Table 6(b): Ratio table of range and mean value (internal friction angle).

Mean value of internal friction angle /°	32.47			
R/°	1.39	3.18	2.37	2.64
α	0.04	0.10	0.07	0.08

It can be seen from Table 6 that the ratio of the cohesive force R of each cohesive force to the mean value of the cohesion of all the tests is significantly higher than the internal friction angle, which indicates that the cohesive force is more sensitive to the change of each factor level under the test conditions, so In the choice of factor level, the influence on cohesion should be given priority. At the same time, it can be seen from the ranking of the primary and secondary factors of the two indicators. For cohesion, the main influencing factors are C and A. That is, the content of blast furnace slag and cement clinker is less sensitive to factors B and D, namely fly ash and desulfurized

gypsum; and for internal friction angle, the above is the opposite. Therefore, C and A factors can be made. Satisfy the optimum level of cohesion, let the B and D factors meet the optimal level of internal friction angle, in order to achieve a better level combination. Therefore, the optimal level combination obtained by the integrated balance method is A3B2C3D3.

For the above test, it can be further analyzed:

(1) Under the same test conditions, the optimal combination of compressive strength is the same as the optimal combination of cohesion, both of which are A3B3C3D1, and the order of primary and secondary factors is similar. A plot of cohesion and compressive strength values to determine the relationship between the two.

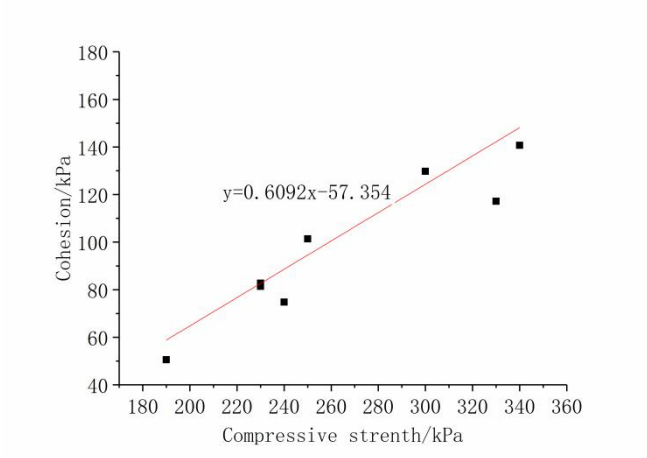

Figure 5: Relationship between cohesion and compressive strength values.

It can be seen from Figure 5 that there is a good linear relationship between the cohesive force and the compressive strength of the test piece, which is consistent with the formula given by the Arioglu strength model [13], which is fitted in the research results of this paper. In the primary curve, the longitudinal intercept D is -57.354 kPa and the slope B is 0.6092. This intrinsic linear relationship exists because the failure of the test block depends on the development of internal micro-cracks. When the test block is subjected to positive pressure, its internal The greater the cohesion, the slower the rate of development of microcracks, the more limited the transverse strain will be, making the test piece less susceptible to damage [14]. This shows that when comparing soil cohesion It can be qualitatively judged by unconfined compressive strength.

(2) The purpose of the direct shear test of the cured sample is to explore the change of the strength property of the curing agent to the ultrafine tailings sand to test the curing effect. As shown in Table 7, the superfine tailings clay cohesion before and after solidification Comparison of changes in internal friction angle.

Table 7: Comparison of cohesion and internal friction angle of ultrafine tailings sand before and after solidification.

Strength index	Original sample	First set of samples	Second set of samples	Third set of samples	Fourth set of samples
Cohesion/kPa	27.00	50.53	74.81	117.16	101.33
internal friction angle /°	25.53	29.41	35.58	32.33	35.17

Table 7(Continued): Comparison of cohesion and internal friction angle of ultrafine tailings sand before and after solidification.

Strength index	Fifth set of samples	Sixth set of samples	Seventh set of samples	Eighth set of samples	Ninth set of samples
Cohesion/kPa	140.70	82.71	129.74	81.42	161.94
internal friction angle /°	33.63	30.78	31.95	33.45	30.00

It can be seen from Table 7 that after the addition of the curing agent, the cohesive force of the ultrafine tailings sand is increased from the original 27.00 kPa to 50.53 to 161.94 kPa, and the internal friction angle is raised from the original 25.53 ° to 29.41 to 35.58 °. Between the two, the curing effect is remarkable. At the same time, it can be seen that when the amount of cementing material is small (1 group of samples, the amount of cementing material is 4.5%), the cohesion and internal friction angle increase values are at a low level. When the amount of cementitious material rises to between 5.75% and 7.00%, the values of cohesion and internal friction angle increase with different degrees of gelling materials. The analysis process has been described in this section. Partial description.

3.3. Penetration Test

The ratio of curing agent selected in this part of the penetration test takes into account the following three aspects:

(1) The amount of curing agent. The amount of curing agent should cover the range of the above test more completely.

(2) Strength index: Under the condition that the curing agent content is similar, the samples with good unconfined compressive strength, cohesion force and internal friction angle are all good.

(3) Evaluation of economic applicability. Cement clinker is an industrial semi-finished product, which is more expensive than industrial waste such as fly ash, blast furnace slag and desulfurization gypsum. Therefore, it is necessary to compare different cement clinker contents as much as possible. The comprehensive characteristics of the sample, in order to reduce the amount of cement clinker appropriately when conditions permit.

Based on the above three considerations, the ratio of curing agent used in this part of the penetration test is the ratio of the first sample, the second sample, the fifth sample and the seventh sample in the above test ratio.

Table 8: Permeability coefficient table of each group.

Test number	Permeability coefficient (cm/s)
Original sample	4.03×10^{-5}
First set of samples	1.61×10^{-05}
Second set of samples	7.12×10^{-06}
Fifth set of samples	5.25×10^{-06}
Seventh set of samples	5.00×10^{-06}

It can be visually seen that the permeability coefficient of the cured sample has a significant downward trend compared to the ultrafine tailings. It can be qualitatively judged by plotting the

relationship between the permeability coefficient and the content of the cementitious material. The relationship between the two is shown in Figure 6.

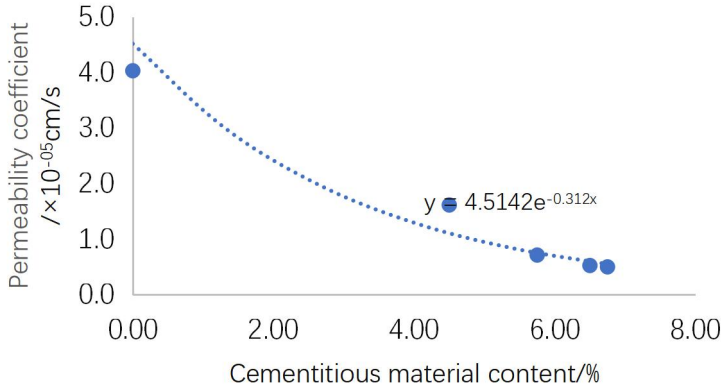

Figure 6: Relationship between permeability coefficient and cementitious material content.

The trend of the permeability coefficient of the four groups of tests with the addition of cementitious materials shows that the decreasing trend of the permeability coefficient gradually becomes slower when the content of the cementitious material is between 4.5 and 7.

The following changes are made to the change of the permeability coefficient caused by the change of the content of the gelling material:

(1) The hydration of the cementitious material glues the originally loose ultrafine tailings together, which reduces the large pores inside the soil and increases the overall compactness [15].

(2) The cementitious material that is not involved in hydration has a small particle size and can be filled into the small pores existing in the system, further affecting the compactness of the tailings sand [15].

(3) Since the amount of cementing material is at a low level, the hydration product cannot completely enclose the particles of the original tailings sand, and the filling effect of the cementing material not participating in the hydration is also limited, so the system After the permeability coefficient is reduced to a certain level, no sudden changes will occur.

The quantitative study on the permeability coefficient of the amount of cementing materials involved in hydration and not participating in hydration is to be further explored in subsequent experiments.

4. Conclusions

In this paper, the orthogonal test of solidification of ultrafine tailings sand was carried out, and the change of soil mechanical properties before and after tailings sand was taken as the main index to comprehensively judge the actual curing effect of each curing agent.

Through the study of the effects of cement clinker, fly ash, blast furnace slag and desulfurization gypsum on the tailings under orthogonal test conditions, the following conclusions can be drawn:

(1) Under the test conditions, for the compressive strength of the 3-day-old tailings sand solidified sample, the optimum curing agent ratio is 3% of cement clinker, 2% of fly ash, 2% of blast furnace slag, and Desulfurization gypsum 1%, the combination number under the test conditions is A3B3C3D3. For the compressive strength of the 7-day-old tailings sand solidified sample, the best curing agent ratio is 3% cement clinker, 2% fly ash , blast furnace slag 2%, and desulfurization gypsum 0.5%, the corresponding combination number under the test conditions is A3B3C3D1.

(2) For the cohesive force and internal friction angle of tailings sand, after taking into account the primary and secondary influencing factors of the two, it is concluded that the best curing agent ratio scheme is cement clinker 3%, fly ash 1.5 %, blast furnace slag 2%, and desulfurization gypsum 3%, the corresponding combination number under the test conditions is A3B2C3D3. After adding the curing agent, the cohesive force of the ultrafine tailings sand is increased from the original 27.00kPa to 50.53~161.94kPa The internal friction angle increased from 25.53° to 29.41~35.58°.

(3) There is a certain positive correlation between the cohesive force of the tailings sand sample after solidification and its uniaxial compressive strength. For this reason, the uniaxial compressive strength can be used to qualitatively compare the cohesive force of the soil sample. Judge.

(4) When the curing agent content range is between 4.5 and 7, the permeability coefficient of the tailings sand will decrease with the increase of the curing agent content, but the downward trend will gradually slow down. This is related to the curing agent for the internal pores of the tailings sand. The filling ability is related.

Acknowledgments

This work is supported by the National Key Research and Development Plan of China(No.2017YFC0804609).

References

[1] Miettinen T, Ralston J, Fornasiero D. The limits of fine particle flotation [J]. Minerals Engineering, 2010, 23(5): 420-437.

[2] Wu Zongzhi, Mei Guodong. Statistical Analysis of Tailings Reservoir Accidents and Causes of Dam Breaking [J]. China Safety Science Journal, 2014, 24(09):70-76.

[3] Kwak M, Jame D F, Klein K A. Flow behavior of tailings paste for surface disposal[J]. International Journal of Mineral Processing, 2005, 77(03): 139-153.

[4] Milton A, Cooke J A, Johnson M S. A comparison of cadmium in ecosystems on metalliferous mine tailings in Wales and Ireland[J]. Water, Air & Soil Pollution, 2004, 153(1/4): 157-172.

[5] Men Yongsheng, Chai Jianshe. China's tailings safety status and accident prevention measures [J].China Safety Science Journal,2009,5(01):48-52.

[6] Tian Wenqi, Xie Xuyang. China's tailings pond status and safety countermeasures [J].China Mine Engineering,2009,38(06):42-49.

[7] Wei Yong, Xu Kaili, Zheng Xin. Analysis of accidents and causes of tailings dams at home and abroad[J].Metal Mine,2009(07):139-142.

[8] Yu Guangming, Song Chuanwang, Pan Yongzhan, et al. New foreign developments in the safety study of tailings dams and the current situation and development trend in China[J].Chinese Journal of Rock Mechanics and Engineering,2014,33(Increase1):3238-3248.

[9] Chen Jie, Yang Zhiqiang, Gao Qian. Test method for the degree of formation of new type of filling material for desulfurization gypsum[J].China Powder Science and Technology,2014,20(06):44-47.

[10] Wang Liqun, Yuan Yongtao, Qi Liqiang. Desulfurization gypsum performance and its comprehensive utilization [J]. Fly Ash Comprehensive Utilization of, 2004 (01): 41-44.

[11] Chang Xiuli. Desulfurization gypsum performance research [D]. Harbin: Harbin Institute of Technology, 2011.

[12] Fan Xianping. The role of activator in gypsum composite cementitious materials and its influence law [D]. Chongqing: Chongqing University, 2013.

[13] Wu Xianghui. Cement Filling Body Strength Model and Application Research [D]. Yunnan: Kunming University of Science and Technology, 2013.

[14] Ye Liping. Concrete Structure (2nd Edition, Volume 1) [M]. Beijing: Tsinghua University Press, 2006.

[15] Suksun Horpibulsuk, Runglawan Rachan, Avirut Chinkukijniwat, Yuttana Raksachon, Apichat Suddeepong. Analysis of strength development in cement stabilize[J]. Construction and Building Materials, 2010, 24: 2011-2021.